AIAA 81-4106

# Load Transfer from a Smooth Elastic Pin to a Large Sheet

S. P. Ghosh,* B. Dattaguru,† and A. K. Rao‡
*Indian Institute of Science, Bangalore, India*

**The plane problem of load transfer from an elastic interference or clearance fit pin to a large elastic sheet with a perfectly smooth interface is solved. As the load on the pin is monotonically increased, the pin-hole interface is in partial contact above certain critical load in interference fit and throughout the loading range in clearance fit. Such situations result in mixed boundary-value problems with moving boundaries and the arc of contact varies nonlinearly with applied load. These problems are analyzed by an inverse technique in which the arcs of contact/separation are prescribed and the causative loads are evaluated. A direct method of analysis is adopted using biharmonic polar trigonometric stress functions and a simple collocation method for satisfying the boundary conditions. A unified analytical formulation is achieved for interference and clearance fits. The solutions for the linear problem of push fits are inherent in the unified analysis. Numerical results highlighting the effects of pin and sheet elasticity parameters are presented.**

## Nomenclature

| | |
|---|---|
| $A_m$ | = free constants in stress functions |
| $2a$ | = diameter of hole |
| $E,G,\nu$ | = elastic constants; Young's modulus, rigidity modulus, and Poisson's ratio |
| $e$ | $= E_p/E_s$ |
| $M$ | = stage of truncation of series |
| $n$ | = number of equidistant points in collocation |
| $P$ | = pin load per unit sheet thickness |
| $p$ | = pin load parameter $E_s a\lambda/P$ |
| $r,\theta$; $X,Y$ | = polar and Cartesian coordinates relative to hole center |
| $R$ | $= r/a$ |
| $U,V$ | = radial and tangential displacements |
| $u,v$ | = displacements in Cartesian coordinates |
| $u_0,v_0$ | = components of rigid body displacements of pin |
| $\gamma$ | = angle between pin load direction and $X$ axis |
| $2\theta_s$, $2\theta_c$ | = arcs of separation or contact |
| $2\theta_p$, $2\theta_p'$ | = arcs of separation or contact for push fit |
| $\lambda$ | = proportional interference between pin and hole = (pin diameter − hole diameter)/hole diameter, takes negative values for clearance |
| $\mu$ | = friction coefficient |
| $\sigma$ | = direct and shear stress with proper subscripts |
| $\tau_{max}$ | = maximum shear stress at a point |
| $\phi$ | = Airy stress function |
| $\psi$ | = displacement function auxiliary to $\phi$ |
| $\sigma_{eq*}$ | = Von Mises equivalent stress, $=\sqrt{(\sigma_r^2+\sigma_\theta^2-\sigma_{r\theta}+3\sigma_{r\theta}^2)}$ |

*Subscripts*

| | |
|---|---|
| $cr$ | = critical, or threshold for initiation of separation or contact |
| $s,p$ | = refer to sheet and pin (except when associated with $\theta$) |
| $x,y,r,\theta$ | = directions associated with load and stress levels |

## Introduction

LOAD transfer through pins with interference, push, or clearance fits occurs in a variety of practical situations. Bolted or riveted lap and lug joints are significant examples.

In this paper, an analytical solution for the load transfer from an elastic pin to a large plane elastic sheet with a perfectly smooth interface is considered including the effects of partial contact along the pin-hole interface. As the load on the pin is monotonically increased the interference pin initially maintains full contact with the hole and at a critical load the pin starts separating from the sheet (closed form solutions are obtained for the state of complete contact in interference fits in the small range of loading). For clearance fit pins, the pin-hole interface maintains only partial contact throughout the range of loading. With monotonically increasing pin load, the arc of contact varies nonlinearly, progressively reducing for interference fit and progressively increasing for clearance fits. Such situations lead to mixed boundary value problems with moving boundaries. These are analyzed by an inverse technique in which the arcs of separation or contact are prescribed and the causative loads are evaluated. A direct method of analysis is adopted using biharmonic polar trigonometric stress functions and simple collocation technique for satisfying the boundary conditions. An elegant unified analytical formulation is achieved for interference and clearance fits. It has been shown that the presentation of numerical data is compact by introducing a pin load parameter $p=E_s a\lambda/P$ and treating the clearance as negative interference. Push fit is an intermediate or transition situation between interference and clearance fit and turns out to be a linear problem. Its solution is inherent in the unified analysis.

Much of the earlier work on these load transfer problems is experimental. Excellent photoelastic studies have been carried out by series of workers[1-4] with special emphasis on the study of stress concentrations around the pin-hole interface. Strain gage techniques too have been adopted for this purpose.[1] By using different materials for the pin and the sheet they could bring in the effects of pin elasticity on the load transfer and concentrations. Some of their results will be discussed in our numerical examples. Reference 3 describes an elegant technique for identifying the load for initiation of separation through a make-and-break circuit with an embedded conducting wire in the sheet.

On the other hand, the analytical studies in the past are few and limited in scope. Venkataraman[5] developed the closed form solutions for the load transfer from rigid interference pins with smooth and slip-free interfaces, in the preseparation range of loading. He had also solved the load transfer in lugs by approximate methods. Martinovich and Shukin[6] also handled the load transfer problem in the preseparation realm in interference fits with elastic bushes in large sheets through Kolosov-Muskhelishvili functions. In

Received Sept. 21, 1979; revision received Aug. 22, 1980. 

*Ministry of Education Research Scholar, Dept. of Aeronautical Engineering (Assistant Professor, R. E. College, Durgapur, West Bengal, on deputation).

†Assistant Professor, Dept. of Aeronautical Engineering.

‡Professor, Dept. of Aeronautical Engineering.

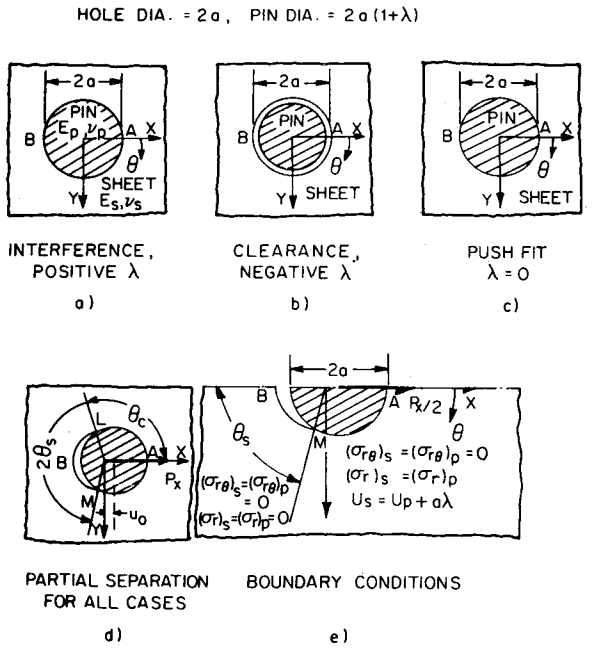


**Fig. 1 Smooth interface: any fit: pin load $P_x$: configuration and boundary conditions.**

these problems some of the Russian achievements till 1973 are described in the work of Kalandiya.[7] Noble and Hussain[8] have made significant theoretical contributions for the study of partial contact behavior. They formulated the plane strain problem of elastic-smooth push-fit pin and obtained dual trigonometric series arising from two distinct boundary conditions on the arcs of separation and contact. Presuming a case of pin and sheet having identical $G/(1-2\nu)$ they could reduce the equations to Fredholm integral equation in terms of unknown contact stresses and angle of separation. After a series of manipulations they could reduce these integral equations to an airfoil equation and obtained solution by Peters'[9] method. For arbitrary materials they have to seek approximate solutions, based on variational methods.

Effective techniques of analysis with a scope to generate extensive numerical information with limited effort were lacking until recently, when Eshwar et al.[10] presented a unified treatment for load transfer from a rigid pin to a large sheet with interference or clearance fit. The present paper is a logical next step in application of this technique for understanding of load transfer from an elastic pin to a large sheet.

## Configuration

We consider an infinite, thin, plane sheet with a hole of diam $2a$. Introduction of a pin of diam $2a(1+\lambda)$ may result in interference, clearance or push fit (Figs. 1a-c). The interface between the pin and the sheet is assumed to be perfectly smooth $[(\sigma_{r\theta})_s=(\sigma_{r\theta})_p=0,\ r=a]$, so as to permit free tangential displacements all around the interface.

Since the pin is deformable (elastic), it is of significance to consider the manner in which the load is applied to the pin. In practice, the pin has a length much larger than the thickness of the sheet to which or from which the load is transferred. During the process of load transfer the pin sits elastically on the hole and bends. This leads to a complete three-dimensional problem, the analysis of which is difficult. However, to have an insight into the phenomenon an idealization of the pin and loading can be made, such that the pin is modelled by a disk of the same thickness as that of the sheet and equivalent line load applied to the disk, leading to a plane-stress problem. Such a postulation is known to result in physically unacceptable infinite stresses and displacements at the center of the pin. To overcome this situation, we can presume loading, either as a body-force distribution corresponding to the actual shear-stress distribution at the ends of the pin, or assume that the core of the pin consists of a bonded concentric rigid circular rod, through which the load is applied. Analytically, the first assumption is close to reality. In the latter case, the core dimension is irrelevant to the analysis recognizing that the stresses in the actual pin are small around its center and it has virtually no effect on stresses and displacements elsewhere. A two-dimensional solution based on either of these assumptions will provide a first order approximation of solution. The present paper is based on the second assumption.

## Interference Fit: Onset of Separation

Due to oversize of the pin, the initial stress state around the hole in the sheet is one of uniform-radial compression and uniform-tangential tension. These uniform radial and tangential stresses are given by

$$\sigma_r=-\sigma_\theta=-E_s\lambda e/e_1,\ \text{at } r=a \tag{1}$$

where

$$e_1=e(1+\nu_s)+(1-\nu_p)$$

The magnitude of these stresses is significantly dependent on relative pin and sheet material properties. If the pin is rigid compared to the sheet ($e=E_p/E_s\to\infty$) the interfacial pressure is maximum and is equal to $-E_s\lambda/(1+\nu_s)$. At the other end, when the sheet is rigid compared to the pin ($e\to 0$), the sheet is unstressed ($\sigma_r=\sigma_\theta=0$).

Now as the pin load $P_x$ is applied and monotonically increased, the compressive interference stresses are relieved around a part of the interface adjacent to $B(\theta=180$ deg) and increased in another part adjacent to $A(\theta=0$ deg) (Fig. 1a).

As long as the pin and the sheet are in complete contact, the stress and displacement fields in the sheet and the pin can be expressed by biharmonic Airy stress functions $\phi_s$ and $\phi_p$ and the corresponding auxiliary displacement functions $\psi_s$ and $\psi_p$, satisfying all the boundary conditions at the interface ($r=a$) and at the far field, viz.,

$$(\sigma_{r\theta})_s=(\sigma_{r\theta})_p=0,\ (\sigma_r)_s=(\sigma_r)_p,\ U_s=U_p+a\lambda\ ;\ \text{on } r=a \tag{2a}$$

$$(\sigma_r)_s,\ (\sigma_{r\theta})_s\to 0;\ \text{as } r\to\infty \tag{2b}$$

and at any $r$ for both pin ($r\le a$) and sheet ($r\ge a$):

$$-2\int_0^\pi(\sigma_r\cos\theta-\sigma_{r\theta}\sin\theta)\,r\,d\theta=P_x \tag{2c}$$

The stress functions and corresponding auxiliary displacement functions[11] for sheet and pin, respectively, are:

$$\phi_s=\frac{P_x a}{8\pi}\left[-4R\theta\sin\theta+2(1-\nu_s)R\ell nR\cos\theta+(1-\nu_s)R^{-1}\cos\theta\right]-E_s\lambda e a^2\ell nR/e_1 \tag{3a}$$

$$\psi_s=-\frac{P_x(1+\nu_s)}{2\pi aR}(\ell nR\sin\theta-\theta\cos\theta) \tag{3b}$$

$$\phi_p=\frac{P_x a}{8\pi}\left[-4R\theta\sin\theta+2(1-\nu_p)R\ell nR\cos\theta-(1-\nu_p)R^3\cos\theta\right]-E_s\lambda a^2 eR^2/2e_1-E_p e u_0 aR\cos\theta \tag{3c}$$

$$\psi_p=-\frac{P_x}{2\pi aR}\left[(1+\nu_p)(\ell nR\sin\theta-\theta\cos\theta)+(1-\nu_p)R^2\sin\theta\right]-2E_s\lambda e\theta/e_1 \tag{3d}$$

where $u_0$ represents the rigid body component of the displacement of the pin along the load direction and the flexibility of the joint is given by

$$E_s u_0/P_x = e_6/8\pi e \tag{4a}$$

where

$$e_6 = e(1+\nu_s)(3+\nu_s) - (1+8\nu_p - \nu_p^2)$$

The radial stress at the interface boundary ($r=a$) is given by

$$\sigma_r = -(P_x/a\pi)\cos\theta - E_s\lambda e/e_1 \tag{4b}$$

The critical load for onset of separation can be found from the condition $\sigma_r = 0$ at $B(r=a,\ \theta = 180$ deg) as

$$(P_x/E_s a\lambda)_{cr} = \pi e/e_1 \tag{5}$$

Or in terms of a pin load parameter $p = E_s a\lambda/P_x$, we can write,

$$p_{cr} = (E_s a\lambda/P_x)_{cr} = e_1/(\pi e) \tag{6}$$

## Clearance Fit: Initiation of Contact

With a clearance fit an infinitesimally small pin load ($\Delta P_x \to 0$) initiates contact of the pin with sheet at $A(\theta = 0$ deg) by a rigid body movement of the pin ($u_0 = -a\lambda$) ($\lambda$ assumed negative for clearance) and the pin and the sheet are stress free until this stage. As the pin load monotonically increases contact progresses on both sides of $A$ [$LA = AM = \theta_c$ (Fig. 1d)].

## Partial Contact Behavior of Interference and Clearance Fits: A Unified Analysis

We now present a unified analysis of partial contact behavior of interference and clearance fits. An inverse technique of analysis is adopted wherein we consider the region of contact $2\theta_c$ (or of separation $2\theta_s$) is known and find the corresponding pin load $P_x$ required to cause such a state. A simple direct continuum method of analysis is utilized.

Let us consider the state when the pin and the sheet have separated over $\pi$ to $\pi \pm \theta_s$ and are in contact over 0 to $\pm\theta_c$. Due to single axis of symmetry ($X$ axis) we consider only one-half of the field ($\theta = 0$ to $\pi$). The boundary conditions in this region are: around the hole ($r=a$) (Fig. 1e),

$$(\sigma_{r\theta})_s = (\sigma_{r\theta})_p = 0;\ 0 \le \theta \le \pi \tag{7a}$$

$$U_s = U_p + a\lambda,\ (\sigma_r)_s = (\sigma_r)_p;\ 0 \le \theta \le \theta_c \tag{7b}$$

$$(\sigma_r)_s = (\sigma_r)_p = 0;\ \theta_c \le \theta \le \pi \tag{7c}$$

and for both pin and sheet,

$$\int_0^{\pi} (\sigma_r \cos\theta - \sigma_{r\theta}\sin\theta)\,d\theta = -P_x/2a \tag{7d}$$

and at far field,

$$(\sigma_r)_s,\ (\sigma_{r\theta})_s \to 0;\ \text{as } r \to \infty \tag{7e}$$

With $\lambda$ positive for interference fit and $\lambda$ negative for clearance fit, the above boundary conditions are applicable to both of them.

To reduce the number of unknown constants in the stress functions for computational ease and economy, we rewrite boundary condition Eqs. (7a-c) as follows:

$$(\sigma_{r\theta})_s = (\sigma_{r\theta})_p = 0,\ (\sigma_r)_s = (\sigma_r)_p = f(\theta);\ 0 \le \theta \le \pi \tag{8a}$$

$$U_s = U_p + a\lambda;\ 0 \le \theta \le \theta_c \tag{8b}$$

$$f(\theta) = 0;\ \theta_c \le \theta \le \pi \tag{8c}$$

Airy stress functions $\phi_s$ and $\phi_p$ and corresponding auxiliary displacement functions $\psi_s$ and $\psi_p$, identically satisfying the boundary conditions Eqs. (7d,e) and (8a), can be written as

$$\phi_s = \frac{P_x a}{8\pi}[-4R\theta\sin\theta + 2(1-\nu_s)R\ell nR\cos\theta + (1-\nu_s)R^{-1}\cos\theta] + E_s\lambda a^2 A_0 \ell nR + E_s\lambda a^2 \sum_{m=2,3,4,\ldots} A_m\left[R^{-m+2} - \frac{(m-1)}{(m+1)}R^{-m}\right]\cos m\theta \tag{9}$$

$$\psi_s = -P_x(1+\nu_s)/2\pi aR(\ell nR\sin\theta - \theta\cos\theta) + 4E_s\lambda \sum_{m=2,3,4,\ldots} A_m R^{-m}\sin m\theta \tag{10}$$

$$\phi_p = \frac{P_x a}{8\pi}[-4R\theta\sin\theta + 2(1-\nu_p)R\ell nR\cos\theta - (1-\nu_p)R^3\cos\theta] + E_s\lambda a^2 A_0 R^2/2 - E_s e u_0 aR\cos\theta + E_s\lambda a^2 \sum_{m=2,3,4,\ldots} A_m\left[R^m - \frac{(m-1)}{(m+1)}R^{m+2}\right]\cos m\theta \tag{11}$$

$$\psi_p = -\frac{P_x}{2\pi aR}[(1+\nu_p)(\ell nR\sin\theta - \theta\cos\theta) + (1-\nu_p)R^2\sin\theta] + 2E_s\lambda A_0\theta - 4E_s\lambda \sum_{m=2,3,4,\ldots} A_m \frac{(m-1)}{m(m+1)}R^m\sin m\theta \tag{12}$$

The arbitrary constants $A_0, A_2, A_3, A_4, \ldots A_m$, the pin load $P_x$ and rigid body component of displacement of pin $u_0$ are to be determined by satisfying the remaining boundary conditions, Eqs. (8b) and (8c). For numerical evaluation the infinite series in $A_m$ is truncated to a suitable finite value $m = M$. A simple equidistant collocation technique is found to be satisfactory for the present numerical analysis.

## Numerical Evaluation

For the numerical evaluation, the boundary condition equations to be programmed for the digital computer take the following form:

Due to $f(\theta) = 0$:

$$-\frac{P_x}{E_s a\lambda}\frac{\cos\theta}{\pi} + A_0 - 2\sum_{m=2,3,4\ldots M} A_m(m-1)\cos m\theta = 0$$

$$\text{in } \theta_c \le \theta \le \pi \tag{13}$$

and due to $U_s = U_p + a\lambda$:

$$\frac{P_x}{E_s a\lambda}\frac{e_6\cos\theta}{8\pi} - A_0 e_1 - \frac{eu_0}{a\lambda}\cos\theta + 2\sum_{m=2,3,4\ldots M} A_m\left[\frac{2m(1+e)-e_2}{(m+1)}\right]\cos m\theta = e$$

$$\text{in } 0 \le \theta \le \theta_c \qquad (14)$$

where $e_2 = e(1-\nu_s) - (1-\nu_p)$.

It is now obvious that $P_x/E_s a\lambda$ (or $E_s a\lambda/P_x$) would provide a suitable independent nondimensional parameter in the study of partial contact behavior both for interference and clearance fits. This had been anticipated earlier from physical considerations.[12,13]

In these series of equations $e$, $\nu_s$, $\nu_p$, $\theta_c$ are specified and $A_0$, $A_2$, $A_3$, $A_4$,.....,$A_m$ and $P_x/E_s a\lambda$ and $u_0/a\lambda$ are determined. Once these constants are known, the stress and displacement fields are determined for any stage of approximation.

A computer program in Fortran IV is written applying the direct collocation procedure for the solution of the above equations $n$ equidistant points are chosen in the interval $\theta = 0$ to $\pi$. At the transition point ($\theta = \theta_c$) we collocate for both conditions Eqs. (13) and (14). If the transition point is coincident with one of these points there are $(n+1)$ equations, otherwise we have $(n+2)$ equations.

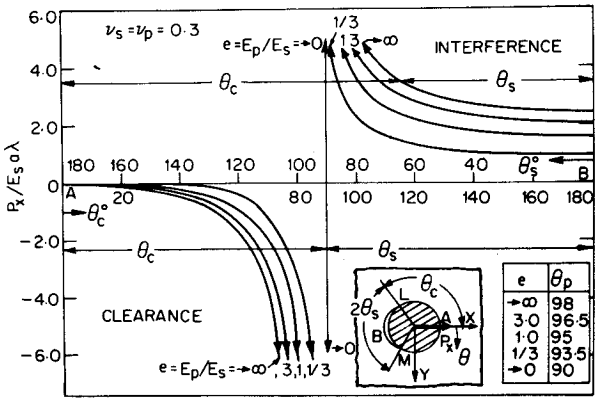


**Fig. 2 Program of separation or contact with increasing pin load $P_x$ for interference or clearance fit joints, smooth interface: effect of pin elasticity.**

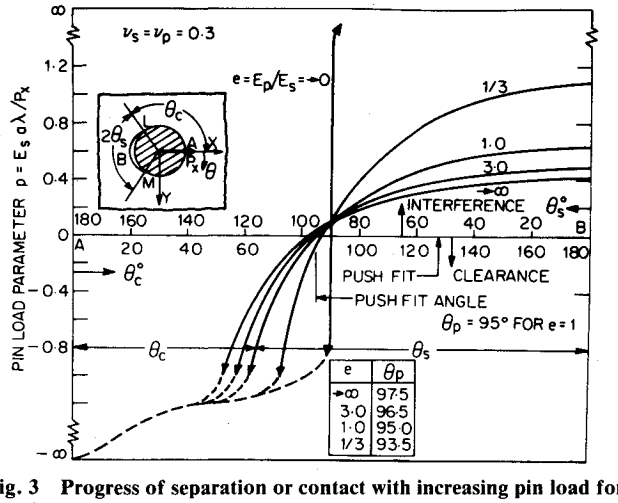


**Fig. 3 Progress of separation or contact with increasing pin load for interference or clearance fit joints, smooth interface: effect of pin elasticity.**

Numerical data are obtained for:

1) $e = 1000,\ 3,\ 1,\ 1/3,\ 0.001$
2) $\nu_s = 0,\ 0.3,\ 0.5$
3) $\nu_p = 0,\ 0.3,\ 0.5$
4) $\theta_c$ = at 10 deg increments from 0 deg to 180 deg
5) $n = 13,\ 25,\ 49,\ 97$

The convergence is excellent in general even with single precision arithmetic only, but tends to be slower for higher loads (i.e., at large separation angles). With $n = 49$, the boundary conditions around the periphery are satisfied within 0.2% of $P_x/a$ or $a\lambda$ as is appropriate.

## Numerical Examples and Discussion

### Load-Contact Variation

*Load-Contact Variation for Identical Pin and Sheet Materials ($e = 1$, $\nu_s = \nu_p = 0.3$)*

Consider the case of the joint with identical pin and sheet material ($e = 1$, $\nu_s = \nu_p = 0.3$). For an interference fit, from Eq. (5), the pin and sheet maintain full contact up to a critical load $(P_x/E_s a\lambda)_{cr} = 1.5707$. At this load separation initiates at point B, Fig. 1d. As the pin load is further increased ($P_x > P_{x,cr}$) the variation of the angle of separation $\theta_s$, with the load $P_x$ is nonlinear, as shown in Fig. 2. With still further increase of load, $\theta_s$ approaches asymptotically to a value $\theta_p$. Numerical evaluation, stipulating angles of separation greater than $\theta_p$ leads to negative values for $P_x/E_s a\lambda$. These negative values correspond to clearance fits ($-ve$ $\lambda$ and $+ve$ $P_x$). The progress of contact in a clearance fit is shown by the clearance

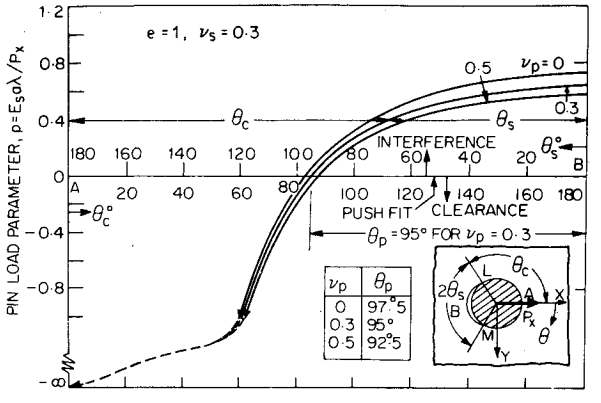


**Fig. 4 Progress of separation or contact with increasing pin load $P_x$ for interference or clearance fit joints, smooth interface: effect of pin Poisson's ratio.**

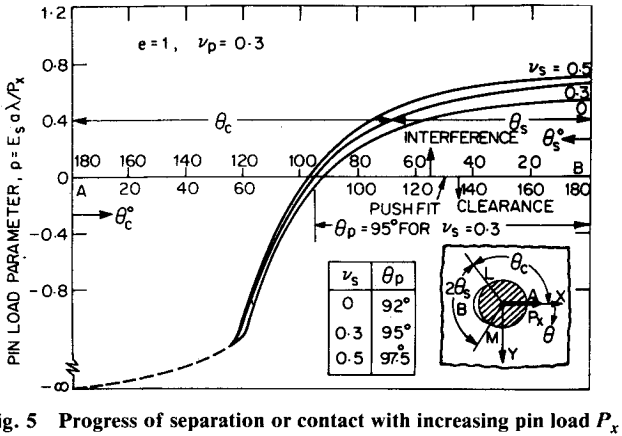


**Fig. 5 Progress of separation or contact with increasing pin load $P_x$ for the interference or clearance fit joints, smooth interface: effect of sheet Poisson's ratio.**

**Table 1 Pin load $P_x$ with smooth interface; push fit semi-arcs of separation $\theta_p$**

| Material properties for pin and sheet $e$ | $\nu_s$ | $\nu_p$ | Semi-arc of separation $\theta_p$, deg[a] |
|---|---|---|---|
| $\rightarrow\infty$ | | | 97.5 |
| 3 | | | 96.5 |
| 1 | | | 95 |
| 1/3 | $(\nu_s=\nu_p=0.3)$ | | 93 |
| $\rightarrow 0$ | | | 90 |
| 1 | 0.3 | 0 | 97.5 |
| 1 | 0.3 | 0.5 | 92.5 |
| 1 | 0 | 0.3 | 92 |
| 1 | 0.5 | 0.3 | 97.5 |

[a] These values are by graphical interpolation and should be accurate to ± ½ deg.

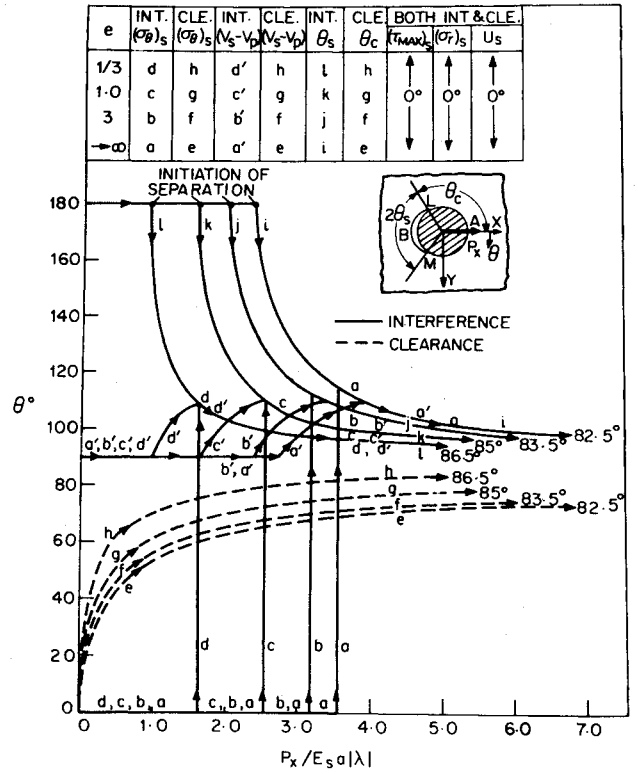


**Fig. 6 Locations of maximum values of stresses and displacements in sheet due to increasing pin load $P_x$: interference or clearance fits, smooth interface.**

curve in Fig. 2. In a clearance fit with infinitesimally small pin load ($\Delta P_x \rightarrow 0$) contact is initiated at $A$ (Fig. 1d). Further increase of pin load causes the contact $\theta_c$ to progress nonlinearly as in Fig. 2. This progress of contact is also limited to an asymptotic value $\theta_p'$, where $\theta_p + \theta_p' = \pi$. For the present case it is seen that $\theta_p = 95$ deg and $\theta_p' = 85$ deg.

From the above information $\theta_p$ and $\theta_p'$ can be determined accurately by replotting a pin load parameter $p(=E_s a\lambda/P_x)$ vs $\theta_s$ or $\theta_c$ as in Fig. 3. In this figure the portion of the curve above the $X$ axis represents interference fit and the portion below, clearance fit. The intersection of the curve with the $X$ axis, i.e., the point $T$ corresponds to $E_s a\lambda/P_x = 0$. Thus at this point $P_x \rightarrow \infty$ for a given $\lambda$ or, alternatively, $\lambda = 0$ for any $P_x$. Thus the angle corresponding to point $T$ represents the angle of separation for a push fit ($\lambda = 0$).

*Effects of Pin-Sheet Material Properties*

The effects of pin-to-sheet modular ratio $e(=E_p/E_s)$ on the load-contact behavior is shown in Fig. 3 for the case of

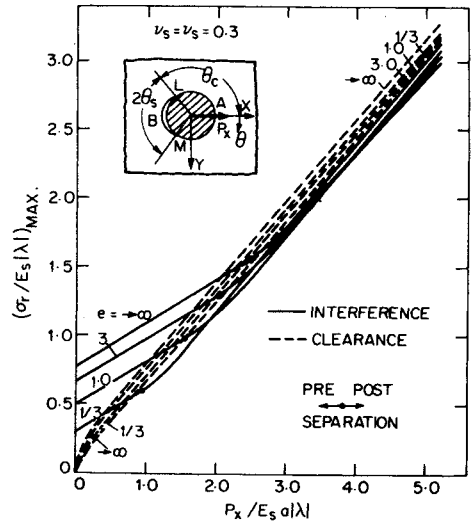


**Fig. 7 Variation of maximum interfacial radial pressure with increasing pin load $P_x$: interference and clearance fits, smooth interface.**

$\nu_s = \nu_p = 0.3$. The curves for five sets of values of $e$, namely $\rightarrow 0, 1/3, 1, 3, \rightarrow\infty$ are shown. 1) The most interesting aspect is that all the curves cross over in the interference portion at $\theta_s = 90$ deg. A separation of 90 deg is achieved for all pin-sheet modular ratios at the same amount of pin load. For a given pin load, a pin with increasing flexibility attains higher angle of separation $\theta_s$ in the range $0 < \theta_s < 90$ deg. In line with this, the load for initiation of separation decreases with increasing flexibility. 2) Above $\theta_s = 90$ deg in a very small region, the trends appear to be reversed. 3) We see that a pin with relative rigidity tending to zero ($e \rightarrow 0$) is not capable of transferring any significant load and due to an infinitesimally small load it separates from the sheet by an angle of 90 deg. Further increase of load does not cause any progress of separation. Again, on the clearance side a pin with zero rigidity makes contact and progresses to $\theta = 90$ deg at an infinitesimally small load.

The effects of the pin-sheet Poisson's ratio ($\nu_s$, $\nu_p$) on the load-contact behavior are shown in Figs. 4 and 5. In Fig. 4 $\nu_p$ is varied keeping $\nu_s$ constant and in Fig. 5 $\nu_s$ is varied keeping $\nu_p$ constant, for $e = 1$. We find that with increasing pin Poisson's ratio the pin tries to adhere to the sheet over larger range of load. On the other hand, with increasing sheet Poisson's ratio, the pin shows the tendency to separate earlier from the sheet. Correspondingly the push fit angles of separation $\theta_p$ decreases.

Table 1 shows the values of semi-arc of separation $\theta_p$ with $e$, $\nu_s$ and $\nu_p$, each time varying one and keeping the other two constant. These values are derived from the graphical plots in Figs. 3-5.

**Stresses and Displacements**

We present here some significant information on stress and displacement fields in sheet in Figs. 6-13 and highlight the salient features.

The maximum hoop stress occurs in the interference fit at $\theta = 0$ deg at small loads, but with increasing load the location jumps to the transition points $M$ or $L(\theta_c)$ (Fig. 6). On the other hand it always occurs at the transition point ($M$ or $L$) for a clearance fit. The locations of maximum radial pressure $(\sigma_r)_{max}$ and the maximum of the maximum shear stress $(\tau_{max})_{max}$ in the sheet along the hole boundary are always at $\theta = 0$ deg for both interference and clearance fits. The variations of these two stress components with load are shown in Figs. 7 and 8, respectively.

The modular ratio $e$ influences the values of the maximum stresses in the sheet significantly in case of interference fit, whereas its effect in clearance fit is very marginal. For an

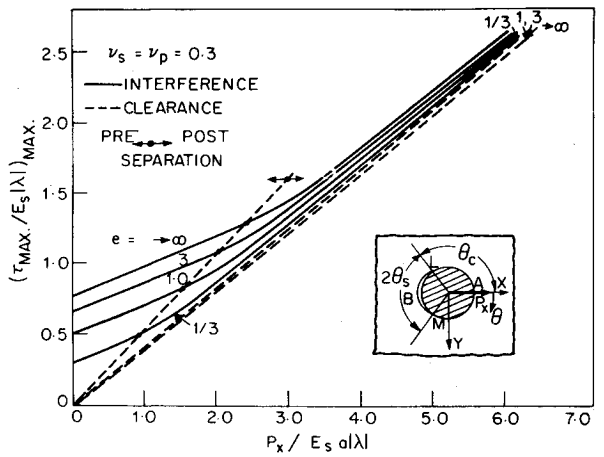


**Fig. 8 Variation of maximum sheer stress in sheet with increasing pin load $P_x$: interference and clearance fits, smooth interface.**

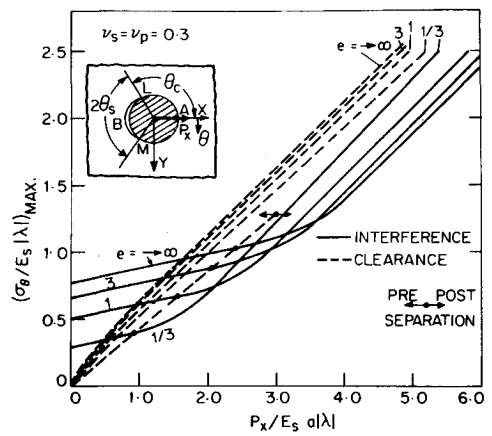


**Fig. 9 Variation of maximum hoop stress in sheet with increasing pin load $P_x$: interference and clearance fits, smooth interface.**

interference fit, in the preseparation realm maximum stresses always occur due to a rigid pin ($e \to \infty$). In the post separation range of loading the trend continues to be the same for $(\tau_{max})_{max}$ and $(\sigma_r)_{max}$, but the trend is reversed in the case of maximum hoop stress $(\sigma_\theta)_{max}$. We find from Fig. 9 that a rigid pin ($e \to \infty$) causes least maximum hoop stress, at large loads. In case of a clearance fit, a rigid pin always leads to maximum hoop stress. The results regarding clearance fit are in conformity with the results reported by Frocht and Hill[1] in 1940. Hoop stresses at other important locations of $\theta = 0$, 90, and 180 deg are shown in Fig. 10 both for interference and clearance fits.

### Interference vs Clearance

A comparison of typical performance curves for interference and clearance fits over a range of elastic moduli can be highly illuminating. Considerind a static design, at lower loads clearance is superior to interference, but a higher loads interference takes over (Figs. 8 and 9). Considering a fatigue design for which alternating stress component (represented by the slope of the curve) is more important than the steady stress component, the interference fit is far superior to clearance fit for any load. In particular, at $\theta = 90$ deg the hoop stress remains constant with load before the onset of separation, so that the alternating component is virtually stifled (Fig. 10).

To assess the onset of yielding in the sheet, we can consider Von Mises yield criterion $\sigma_{eq} = \sqrt{(\sigma_r^2 + \sigma_\theta^2 - \sigma_r\sigma_\theta + 3\sigma_{r\theta}^2)}$ for ductile materials.( $\sigma_{eq})_{max}$ always occurs at $\theta = 0$ deg. Plots of $(\sigma_{eq})_{max}$ vs applied load $P_x$ are shown in Fig. 11. Throughout the loading range we find that clearance fit has lesser $(\sigma_{eq})_{max}$ so that to avoid yielding in the sheet the interference joint

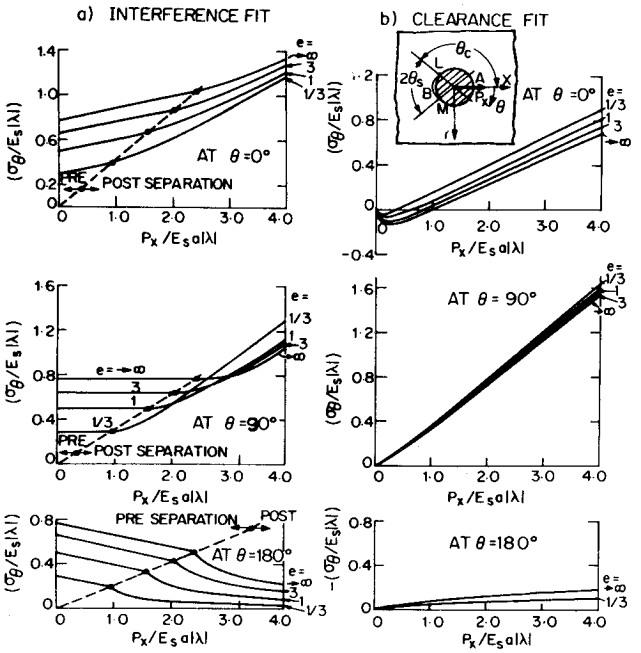


**Fig. 10 Variation of hoop stress in sheet at locations $\theta = 0$, 90, and 180 deg with increasing pin load $P_x$: interference and clearance fits, smooth interface.**

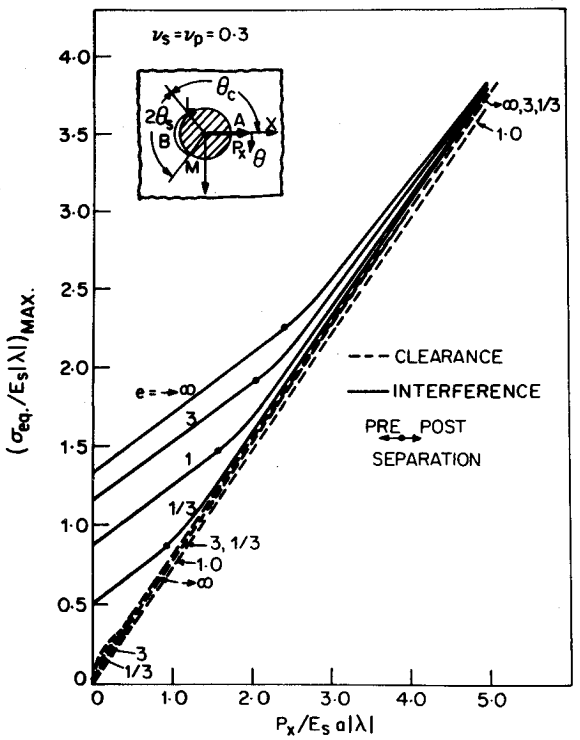


**Fig. 11 Variation of maximum Von Mises equivalent stress in sheet with increasing pin load $P_x$: interference and clearance fits, smooth interface.**

should be operated at a smaller load range as compared to clearance for the same material of the sheet. With interference fit, at small loads a rigid pin causes a maximum of $(\sigma_{eq})_{max}$, but at higher loads curves for all $e$ values converge. But in case of clearance fit, the $(\sigma_{eq})_{max}$ is lowest for only $e = 1$. For any other $e$ ($e \gtrsim 1$) we find that $(\sigma_{eq})_{max}$ is higher and at higher load all the curves practically collapse to a single curve.

### Displacements

Maximum relative tangential displacement $(V_s - V_p)/a\lambda$ in contact region for interference occurs at $\theta = 90$ deg up to a

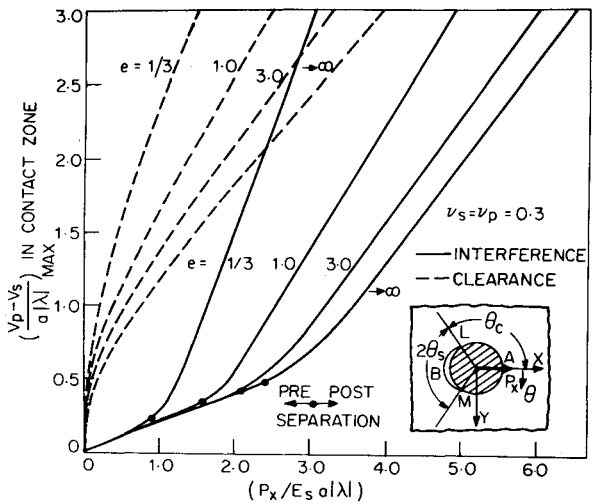


**Fig. 12 Variation of maximum relative tangential interfacial displacement in contact zone with increasing pin load $P_x$: interference and clearance fits, smooth interface.**

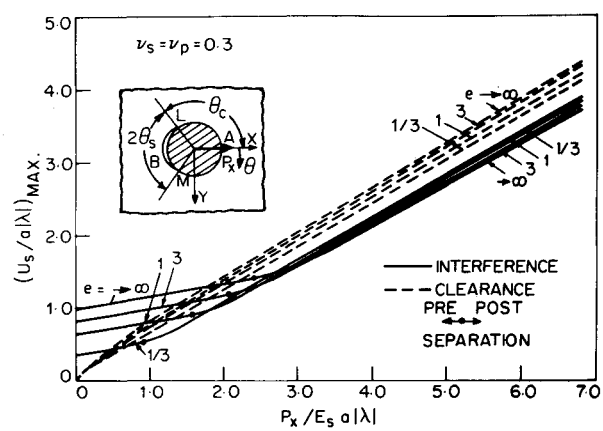


**Fig. 13 Variation of maximum radial displacement in sheet at interface with increasing pin load $P_x$: interference and clearance fits, smooth interface.**

particular load and later on gradually shifts to the transition points $M$ or $L(\theta_c)$. Figure 12 shows the plots for maximum relative interfacial tangential displacements in a contact region. One can observe the influence of modular ratio $e$ in causing a substantial reduction of $(V_s - V_p)/a\lambda$ with increasing $e$.

Maximum radial displacement in sheet occurs at $\theta = 0$ deg for both the joints (Fig. 6). Though interference causes larger maximum radial displacements at smaller loads than clearance fit (Fig. 13), we find that the trend is generally reversed with increasing load. In the preseparation realm (interference fit) the effect of modular ratio is significant, but at higher loads its effect is very small.

## Conclusion

In this paper we have achieved a very satisfactory unified method of analysis for both smooth interference and clearance fit joints with elastic pins under pin load. One of the major benefits of the unified analysis is that the solution of the push-fit problem is inherent in the analysis. Apparently, for the first time a clearance fit with elastic pin is mathematically analyzed. It has been shown that the general stress levels are lower in a clearance fit and it is better than interference fit for a static-stress design. On the other hand, for a fatigue design, local alternating stress components are of paramount significance, and interference fits are far superior to clearance fits.

## References

[1] Frocht, M. M. and Hill, H. N., "Stress Concentration Factors Around a Central Circular Hole in a Plate Loaded through Pin in a Hole," *Journal of Applied Mechanics, Transations of ASME,* Vol. 62, March 1940, pp. A5-A9.

[2] Jessop, H. T., Snell, C. and Hollister, G. S., "Photo-elastic Investigations on Plates with Single Interference Fit Pins with Load Applied to (a) Pin only and (b) Pin and Plate Simultaneously," *Aeronautical Quarterly,* Vol. 9, May 1958, pp. 147-163.

[3] Lambert, T. H. and Brailey, R. J., "The Influence of the Coefficient of Friction on the Elastic Stress Concentration Factor for a Pin Jointed Connection," *Aeronautical Quarterly,* Vol. 13, Feb. 1962, pp. 17-29.

[4] Cox, H. L. and Brown, A. F. C., "Stresses Round Pins in Holes," *Aeronautical Quarterly,* Vol. 15, Nov. 1964, pp. 357-372.

[5] Venkataraman, N. S., "A Study into the Analysis of Interference Fits and Related Problems," Ph.D. Thesis, Indian Institute of Science, Bangalore, India, 1966.

[6] Martinovich, T. L. and Shukin, V. S., "Action of a Concentrated Force on an Elastic Ring Pressed into a Circular Hole in an Isotropic Plate" *Prikladnaya Mekhanika,* Vol. 8, No. 10, 1972, pp. 118-122, (in Russian).

[7] Kalandiya, A. I., *Mathematical Methods of Two-dimensional Elasticity,* English Translation by M. Kowyaeva, Mir Publishers, Moscow, 1975.

[8] Noble, B. and Hussain, M. A., "Exact Solution of Certain Dual Series for Indentation and Inclusion Problems," *International Journal of Engineering Sciences,* Vol. 7, No. 11, 1969, pp. 1149-1161.

[9] Peters, A. S., *Communications in Pure and Applied Mathematics,* Vol. 16, 1963, pp. 57-61.

[10] Eshwar, V. A., Dattaguru, B. and Rao, A. K., "Partial Contact and Friction in Pin Joints," Aeronautical Research and Development Board, Govt. of India, ARDB-STR-5010, Dec. 1977.

[11] Coker, E. G. and Filon, L. N. G., *A Treatise on Photo-elasticity,* Cambridge University Press, 1931.

[12] Rao, A. K., "Elastic Analysis of Pin Joints," *Computers and Structures,* Vol. 9, No. 2, 1978, pp. 125-144.

[13] Ghosh, S. P., "Analysis of Joints with Elastic Pins," Ph.D. Thesis, Indian Institute of Science, Bangalore, India, 1978.